

# Optimization of Endoscopic Video Stabilization by Local Motion Exclusion

Thomas Gross, Navya Amin, Marvin C. Offiah, Susanne Rosenthal, Nail El-Sourani  
and Markus Borschbach

*Competence Center Optimized Systems, University of Applied Sciences (FHDW),  
Hauptstr. 2, 51465 Bergisch Gladbach, Germany*

**Keywords:** Endoscopy, Foreground Moving Objects, Global Motion, Local Motion, Outlier Rejection, Image Composition, Video Stabilization.

**Abstract:** Hitherto video stabilization algorithms for different types of videos have been proposed. Our work majorly focuses on developing stabilization algorithms for endoscopic videos which include distortions peculiar to endoscopy. In this paper, we deal with the optimization of the motion detection procedure which is the most important step in the development of a video stabilization algorithm. It presents a robust motion estimation procedure to enhance the quality of the outcome. The outcome of the later steps in the stabilization, namely motion compensation and image composition depend on the level of precision of the motion estimation step. The results of a previous version of the stabilization algorithm are here compared to a new optimized version. Furthermore, the improvements of the outcomes using the video quality estimation methods are also discussed.

## 1 INTRODUCTION

As discussed in (Offiah et al., 2012) endoscopic videos include a variety of distortions making it difficult for the surgeon to have a better view of the region of interest. These may be the movement of the organs, foreground moving objects such as scalpels, or body fluids secreted during the operation. Of all the distortions, the foreground moving objects contribute majorly to affect the quality of stabilization. This is because, the endoscopic videos have the camera lens held very close to the region of interest. Thus the foreground objects consume major part of the captured video frame. In contrast to the global motion, wherein each image pixel (px) from frame to frame experience the same speed and direction, the direction and speed of the local motion in a local area is different from the co-existing motion in the frame. The estimated motion from our previous motion estimation procedure is majorly influenced by these foreground moving objects. This makes it essential to separate these local motions from the global motion to determine a global camera path for further stabilizing the video. In the following, approaches for local motion detection are presented. Depending on the application field, this research area is sometimes referred to as foreground object detection (Liyuan Li et al., 2003) or local mo-

tion segmentation (Flores-Mangas and Jepson, 2013), (Bradski1 and Davis2, 2002).

## 2 PREVIOUS WORK

The local motion detection plays an important role in a variety of fields, namely object tracking, video surveillance or in the field of video coding (MPEG) (Berna and Faouzi, 2000), (Georgia et al., 2009). Previous approaches for segmentation of local image changes included the subtraction of consecutive video frames where stationary background objects remain in the same position and moving objects change their position from frame to frame. The image frames are then subtracted and only areas with a local change appear in the resultant image. However, this method has the disadvantage that the camera must be located at a fixed position, so that the background is always in the same position. For this reason, this method proved to be unsuitable for our purpose.

Another method for motion detection is to use the optical flow (OF) field, which determines motion vectors for all image px based on the image intensities (Shafie et al., 2009). Motion vectors with different directions and lengths represent the local changes in

the video frame. The exact calculation of the optical flow is limited by the following restrictions: First, the image intensities may differ slightly between successive frames which is not often the case in endoscopic videos. Second, because of the small light source of the endoscope, the lighting conditions often vary within a video sequence. A further disadvantage of the OF is that large movements in the image cannot be well determined. But motion changes in endoscopic recordings can be quite large. Also, the frames must be noise-free, which is not the case in endoscopic videos.

Another technique for motion detection is the feature-based method, which detects feature points in a frame and tracks the feature points in the next frame (Han et al., 2006). This method is well suited for this approach of this work because it is based on feature points. The local motion detection can be directly integrated into our video stabilization algorithm Endostabf2f.

### 3 MOTION ESTIMATION

The process of video stabilization includes three major steps: motion estimation, motion compensation and image composition. The quality of the resultant video completely depends on the precision of these three steps. However, motion estimation influences the quality majorly. The process of estimating motion vectors from the extracted features is influenced by certain distractions which need to be dealt with to obtain the optimal motion vectors. To do so, the following approaches are used to first exclude the outliers and further the local motion vectors to attain the global camera path:

#### 3.1 Outlier Removal

Feature detection using Shi-Tomasi corner detection algorithm (Shi and Tomasi, 1994) and looking for matching features in the next frame using KLT tracker (Kanade-Lucas-Tomasi feature tracker) (Tomasi and Kanade, 1991) generate point matches tracking the best match for spatial intensity information. However, changes in the corresponding frame such as luminance variations, out of plane rotations lead to some false matches called 'outliers' which corrupt the results of stabilization. This complicates the estimation of geometric transformation leading to jittery videos with added shakes. Some of these irregularities can be solved by performing an outlier rejection method using RANSAC (Zhao et al., 2009) on the corresponding point matches. Figure 1 shows the results of the

RANSAC outlier analysis and removal. The image on the left shows two frames, current and next overlaid on each other. The red circles and green crosses represent the features and the connecting yellow lines show matching features between the two images. The left image shows some false matches between distant points in the respective frames. The image on the right of Figure 1 shows perfect matches left after the application of the outlier removal procedure.

#### 3.2 Local Motion Detection

Our motion estimation approach algorithm includes local motion detection and foreground moving object detection. In the first step, the image is divided into  $m \times n$  large sectors called grid cells. The feature points (FPs) determined in the subsequent steps are assigned to a cell and the local movement of a cell is measured. Different cell sizes can be selected and typically a size of  $10 \times 10$  px is used. Since the video recordings have different resolutions such as  $384 \times 288$  px to  $1280 \times 1024$  px for HD videos, the cell size can be chosen dynamically, depending on the image resolution. Once the FPs were determined using the KLT method in frame A and tracked in frame B, the untraceable FPs are deleted from the feature point matrix. As a result, only valid FPs, which correspond in the two frames, are kept (Frame A: reference points, Frame B: tracked points). Next, all the FPs are assigned to their respective grid cell. An index matrix is created to indicate the cell belonging to its respective FP. Then, the local motion for individual cell is determined by calculating an average of motion values from all FPs within the respective cell. More specifically, the change of the x and y position from frame A to frame B for each FP within a cell  $c_i$  is measured.

The change of the position of each image px represents the movement in a frame. The median of all measured x- and y changes is calculated for each cell and stored in a local cell movement matrix. Cells with too large local translation in the + / - or x + / - y directions, are marked as outliers by using the Median Absolute Deviation from the median (MAD). MAD is a robust estimate of the spread, and calculates the maximum permissible deviation of the position (+ / - x and y) of a cell compared to the overall movement of all the cells in the x or y direction. The MAD is defined as follows (Walker, 1999):

$$MAD = \text{median}_i |c_i - \text{median}_j(c_j)| \quad (1)$$

where,  $c_i$  is motion of an individual cell and  $c_j$  is the set of motion values of all cells.

The cells labelled as outlier cells are excluded from the calculation of the global camera path. In Figure 2 the left image with the red vector arrows show

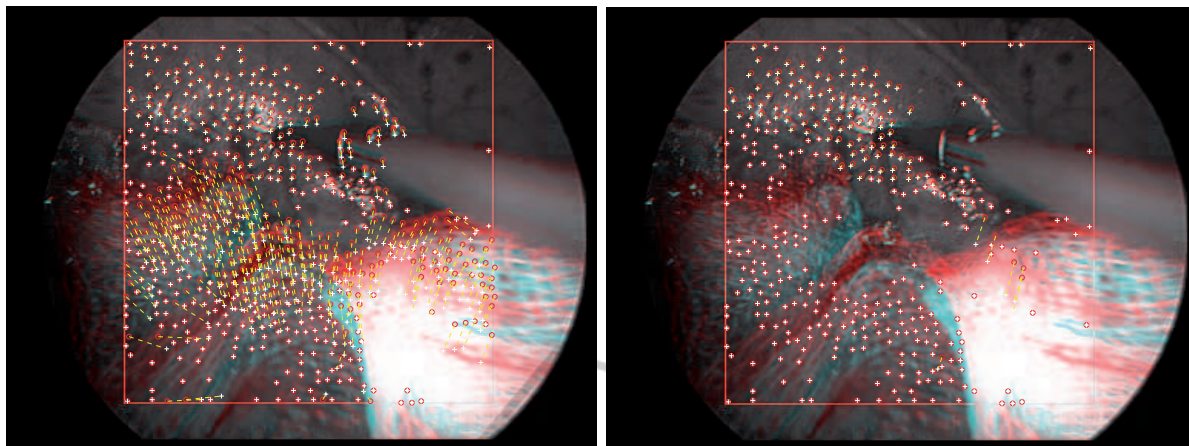


Figure 1: Outlier Rejection. Left: Original image consisting of outliers Right: Resultant one after filtering.

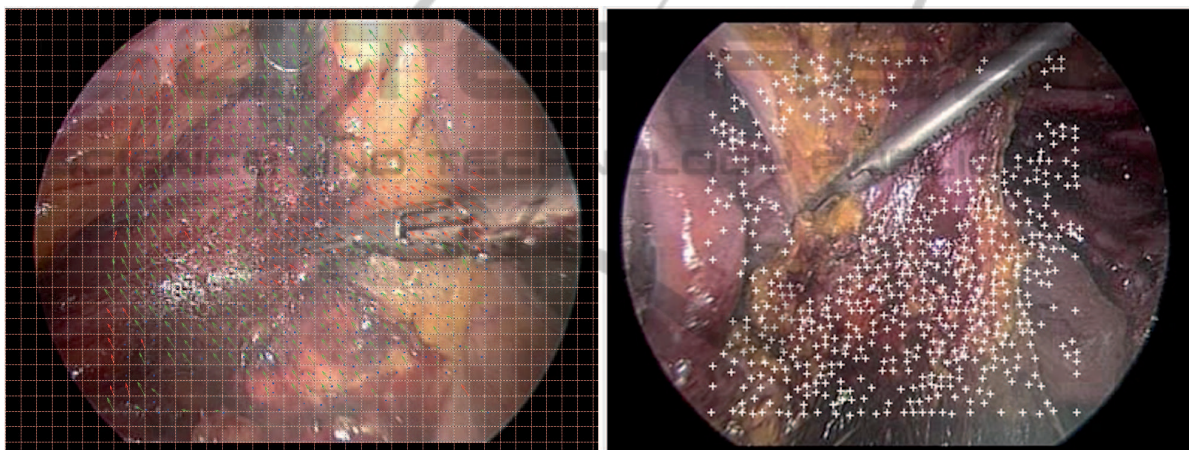


Figure 2: Local motion estimation. Left: Grid Map with global and local motion vectors from the tracked FPs. The red arrows on the moving scalpel are the excluded local motions. Right: FPs after local motion exclusion.

the local movements of the scalpel. In contrast, the green vector arrows represent the movements of the camera. The local motions are excluded for global motion estimation as shown in the right image of Figure 2, where the tracked feature points of a video are represented by white crosses. In the region of the moving scalpel illustrated by red arrows, only local movements are detected by the algorithm and the FPs in this region are excluded from the complete set of tracked FPs. From the  $x/y$  translation values from all inlier cells, the median is calculated, which represents the global camera motion of the endoscope as shown in Figure 3 for the  $y$  direction. The  $Y$ -axis of the graph describes the motion of the  $px$  in the  $y$  direction, the  $X$ -axis indicates the frame number in the video.

Unlike our previous method of motion compensation where we smoothed the raw global camera path and further used this smoothed path for image composition, our current method uses an optimized approach. Here the difference between the original camera mo-

tion and the smoothed camera path is used for image composition. In most cases, the intense movements are in the range of  $\pm 15$  px called the high-frequency jitter. The peaks in the motion curve caused by sudden movement of the endoscope (Figure 4) result in a jerky stabilized video which can be a disadvantage for the subsequent creation of the cropping mask (see next section Image Composition 4). In order to mitigate the impact of these peak values, the values which are above a selected threshold are smoothed. As a threshold  $\pm 12$  px is chosen. To sort out the peak values, the difference curve between the original and smoothed camera motion is calculated as shown in red in figure 4. Thereafter, the difference curve is smoothed where the peak values are reduced as shown in figure 6. Subsequently, all the values in the difference curve (red) which exceed the threshold value are replaced by the values of the smoothed difference curve (green curve). The blue curve in Figure 6 shows the new difference motion

which is used for the transformation in the subsequent image composition procedure.

## 4 IMAGE COMPOSITION

As mentioned in the previous section the smoothed difference curve is used for transformation of the video frames. Affine transformation, in spite of having two added degrees of freedom when compared to Similarity Transformation does not produce expected results as mentioned in (Grundmann et al., 2011), (Zhou et al., 2013). We used the similarity transformation for transforming the video frames according to the smoothed difference curve. Further the frames are cropped such that the stabilized video is devoid of black borders which are a result of the motion compensation. In the previous step, the motion values in the video are reduced to a maximum allowed value. This makes it possible to calculate a cropping mask, which discards the black area around the stabilized video. The maximum movement in the video is the maximum value used for the cropping area. However, it would be better to divide the video into scenes and not crop the entire video with the maximum value because individual scenes often have different movements.

## 5 EXPERIMENT

The complete workflow of the stabilization process is described in detail in (Amin et al., 2014). The motion estimation part of the previous algorithm described in this paper is optimized by excluding the

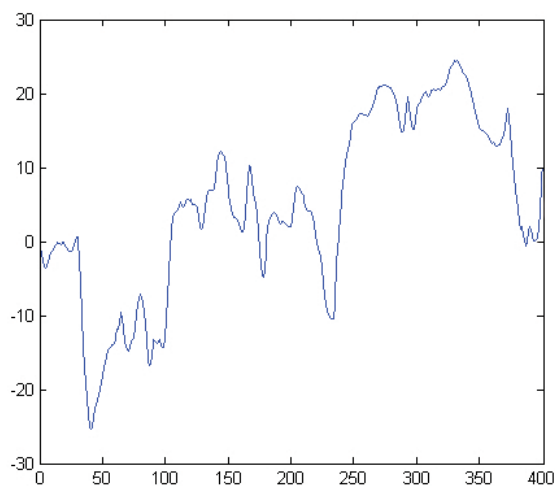


Figure 3: Camera motion (Pixel) in y-direction over 400 frames.

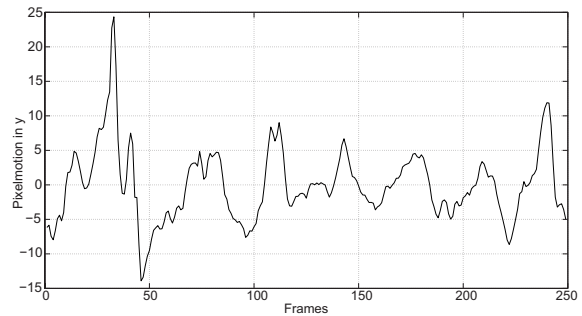


Figure 4: Difference of motion between Original Global Camera Motion and Smoothed Global Camera Motion.

local motion vectors in the current Endostabf2f\_LME algorithm. The stabilization algorithm EndoStabf2f with Local Motion Exclusion (LME) and without LME is applied to two datasets: Dataset 1 including 15 non-distortion-specific videos (provided by the Forschungszentrum Borstel (Frey, 2012) and Leipzig (HTWK Leipzig, 2013)) and dataset 2 including 52 gastroscopic distortion-specific test video sequences from human surgery that were provided by the Charité Berlin (Charité Berlin, 2013).

The test video sequences of dataset 2 were taken from a large database of over 1400 videos. These videos are of varying file sizes, durations and frame numbers and have a resolution of 364x288 px (including, in part of the cases, black regions around the medical ROI), while the medical ROI generally covers at least three quarters of each video frame. They are available as MPEG files and are converted to MP4 (25 frames and 2208 kb per second). A list of 11 different distortion types (see appendix) is defined that follows from the previously described and referenced types of distortions in endoscopic videos. The 1400 videos are also manually screened to identify further distortion types that flow into this list. A second manual screening process by members of the scientific team goes through each distortion type of this list and identifies appropriate videos that contain that distortion type. This categorization of video scenes by distortion type enables a distinguished (distortion-specific) evaluation of the stabilization algorithm.

It is of course the case that multiple distortion types occur in some video scenes (or in parts of them) although only associated with a particular distortion type in its test case (e.g. a video with foreground objects that also contains smoke and body fluids). (It is of course also not excluded that the same video source is used for several test cases, be it with different scenes.) This can generally not be prevented but compensated for by increasing the sample size (i.e. the number of test cases and scene lengths) per distortion type. At the same time, the high computation

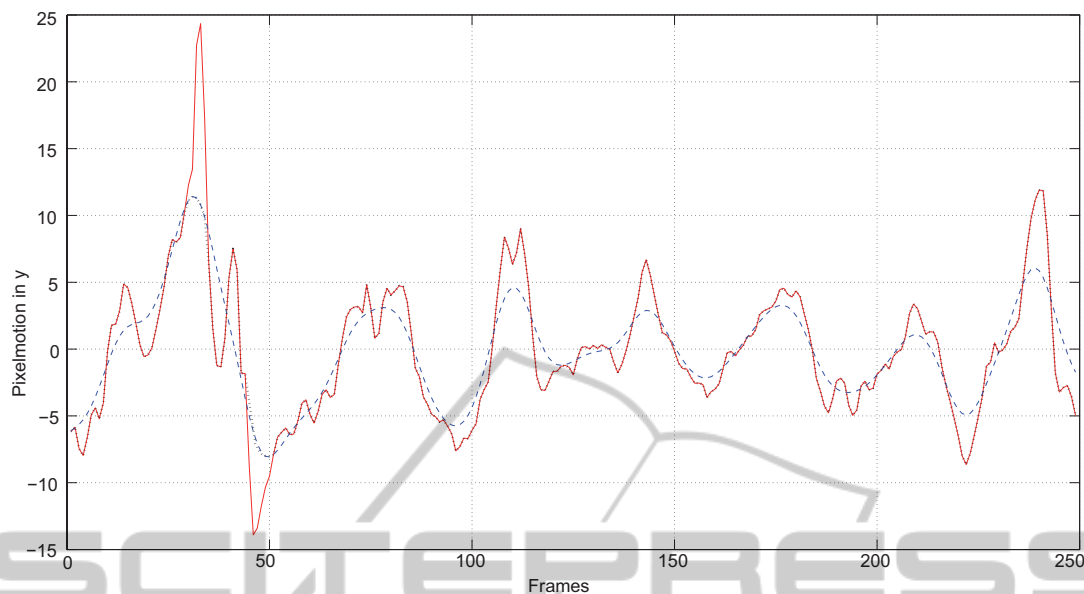


Figure 5: Difference of motion between Original Global Camera Motion and Smoothed Global Camera Motion (solid line), Smoothed difference curve (dashed) and replaced peak values used for the Image Composition (dotted).

time of the stabilization algorithm (which at this level is not optimized for runtime performance) sets some limits on the number of frames that can be stabilized in a justifiable time. For this reason, the screening of the over 1400 videos only selects 5 test cases per distortion type. As an exception, only two scenes are used for the Low Light distortion type. See the appendix for a full list of all distortion types, the number of videos used in each, and their respective cumulative number of frames used for the stabilization and quality calculation. This adds up to 52 test cases comprising approximately 69,000 frames.

For dataset 1, both the LME and non-LME algorithms are applied. The robustness of the Endostabf2f\_LME is further tested on distortion-specific videos of dataset 2 (i.e., only the non-LME version is used there). The stabilization of all videos is carried out in Matlab. Each test case first calculates the binary ROI mask described earlier. Only content within this video mask is considered during feature detection, and after the final warping of each frame, the mask is applied to the frame before writing it into the stabilized output video. This makes the output video also visually stable, as it prevents a visually unstable ROI (except for the resulting black areas within the mask).

## 6 RESULTS AND DISCUSSION

The benchmarking of the algorithm is done by using the Inter-Frame Transformation Fidelity (ITF) (Mormotoa and Chellappa, 1998) where an average PSNR

is calculated between consecutive frames across the whole video. For dataset 1, the results of Endostabf2f with LME is compared to the results of Endostabf2f without LME and evaluated per video. The videos of data set 1 that are stabilized using the Endostabf2f with LME, shows better quality (i.e. higher PSNR values) compared to the stabilized videos using the Endostabf2f with the LME. As shown in Figure 6, the endoscopic videos with heavy foreground movements show a very high difference in quality for the Endostabf2f\_LME compared to the other with higher PSNR values. This shows that excluding the local motion from the estimation of the global camera motion does have a positive impact on the overall quality of the stabilized videos.

For dataset 2, the PSNR metric both for the original (unstabilized) video scene and for the stabilized one are calculated to identify their improvements across different distortion types as follows: The metric is first calculated for every original and stabilized video scene of a test case: PSNR for neighbouring frames of the test scene (i.e. between neighbouring frames in the intervals between start and end frame according to the test database) is determined. PSNR is calculated as shown in the ITF calculation in (C.Offiah et al., 2012). An average PSNR value for all frames of the original and stabilized video, respectively, is then calculated. Next, the distortion-specific PSNR value is obtained by using a weighted average from all test cases pertaining to the specific distortion, where the scene lengths of the associated videos in numbers of frames are used as weights. The results

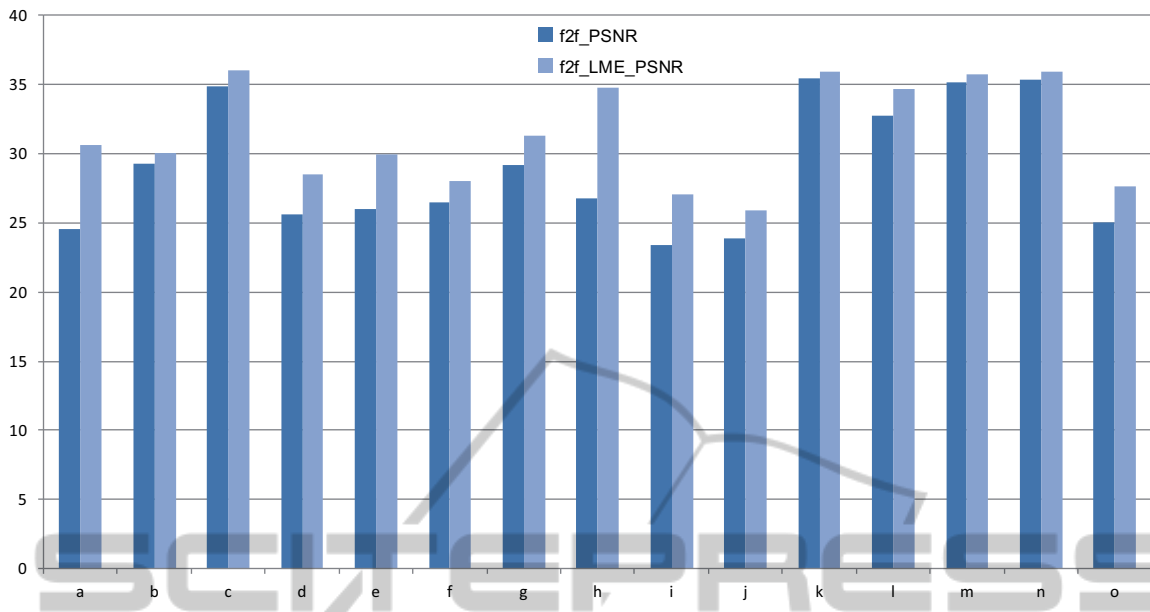


Figure 6: Estimated video quality using PSNR.

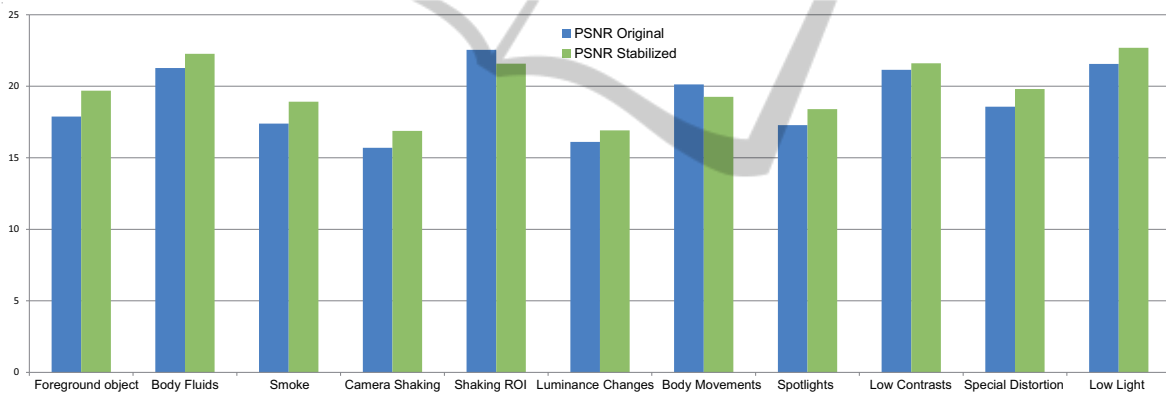


Figure 7: Comparison of the calculated PSNR values in dB for the original and the stabilized videos.

as shown in Figure 7 show that some dB of improvements of the original video are made by using the non-LME algorithm. This holds for most distortion types, with only a shaking ROI and body movements as an exception. This further underscores the conclusions drawn from dataset 1, that non-LME achieves an overall improvement of the video quality.

The exclusion of local motion vectors makes the algorithm robust against presence or absence of immense foreground moving objects. As shown in Figure 8, a comparison between Endostabf2f\_LME (LMV in the figure) and state-of-the-art stabilization algorithms is made along frames from a scene where some internal body movements and no foreground moving objects are present as well as the endoscope moves slightly for examination. In such a case, the Adobe AE shows tremendous frame jump unlike En-

dostabf2f\_LME and YouTube. Youtube also does some scaling and cropping and thus loses some region as seen along the bottom right-hand corner of the frames which might have some useful information for the surgeon. But these problems are dealt well by the Endostabf2f\_LME. Further, in Figure 9, the scene contains introduction and rigorous movement of a forcep. In such a case, again a frame jump is seen in the stabilized frame number 675 for the Adobe AE which could be because of the loss of trajectory on scene change. Endostabf2f\_LME handles problems specific to endoscopic videos well. However, there is still scope for improvement in motion estimation and handling foreground moving objects when these objects consume major part of the frame making it difficult for the stabilization algorithm to distinguish foreground and background.

## ACKNOWLEDGEMENTS

This work as a part of the PENDOVISION-project is funded by the German Federal Ministry of Education and Research (BMBF) under the registration identification 17PNT019. The financial project organization is directed by the Research Center Jülich. The work was conducted under supervision of Markus Borschbach.

## REFERENCES

- Amin, N., Gross, T., Offiah, M. C., Rosenthal, S., El-Sourani, N., and Borschbach, M. (2014). Stabilization of endoscopic videos using camera path from global motion vectors. In *To appear in the 9th International Joint Conference on Computer Vision, Imaging and Computer Graphics Theory and Applications*.
- Berna, E. and Faouzi, K. (2000). Partitioning of video objects into temporal segments using local motion information. In *ICIP*, pages 945–948.
- Bradski, G. R. and Davis, J. W. (2002). Motion segmentation and pose recognition with motion history gradients. In *Machine Vision and Applications*.
- Charité Berlin (2013). Universitätsmedizin Berlin. <http://www.charite.de>.
- C.Offiah, M., Amin, N., Gross, T., El-Sourani, N., and Borschbach, M. (2012). Towards a benchmarking framework for quality-optimized endoscopic video stabilization. In *ELMAR, Sep., 2012 Proceedings*, pages 23–26.
- Flores-Mangas, F. and Jepson, A. D. (2013). Fast rigid motion segmentation via incrementally-complex local models. In *IEEE Conference on Computer Vision and Pattern Recognition*.
- Frey, A. (2012). Research center borstel - leibniz center for medicine and biosciences, germany. <http://www.fz-borstel.de/cms/index.php>.
- Georgia, A. M., Alexander, G., Andreas, K., Thomas, S., Marta, M., and M., K. A. (2009). Global motion estimation using variable block sizes and its application to object segmentation. In *WIAMIS*, pages 173–176.
- Grundmann, M., Kwatra, V., and Essa, I. (2011). Auto-directed video stabilization with robust 11 optimal camera paths. In *IEEE Conference on Computer Vision and Pattern Recognition (CVPR)*.
- Han, M., Xu, W., and Gong, Y. (2006). Video foreground segmentation based on sequential feature clustering. In *18th International Conference on Pattern Recognition, ICPR 2006.*, volume 1, pages 492–496.
- HTWK Leipzig (2013). Forschungszentrum. <http://www.htwk-leipzig.de>.
- Liyuan Li, W. H., Gu, I. Y., and Tian, Q. (2003). Foreground object detection from videos containing complex background. In *In Proc. of the eleventh ACM international conference*.
- Morimoto, C. and Chellappa, R. (1998). Evaluation of image stabilization algorithms. In *Proc. IEEE International Conference on Acoustics, Speech and Signal Processing*, 5:2789–2792.
- Offiah, M. C., Amin, N., Gross, T., El-Sourani, N., and Borschbach, M. (2012). On the ability of state-of-the-art tools to stabilize medical endoscopic video sequences. In *MedImage 2012, Mumbai*.
- Shafie, A. A., Hafiz, F., and Ali, M. H. (2009). Motion detection techniques using optical flow. In *World Academy of Science, Engineering and Technology*.
- Shi, J. and Tomasi, C. (1994). Good features to track. In *IEEE Conference on Computer Vision and Pattern Recognition*, pages 593–600.
- Tomasi, C. and Kanade, T. (1991). Detection and tracking of point features. In *Carnegie Mellon University Technical Report CMU-CS-91-132*.
- Walker, J. T. (1999). *Statistics in Criminal Justice: Analysis and Interpretation*. Aspen Publishers Inc.
- Zhao, F., Wang, H., Chai, X., and Ge, S. (2009). A fast and effective outlier detection method for matching uncalibrated images. In *ICIP*, pages 2097–2100.
- Zhou, Z., Jin, H., and Ma, Y. (2013). Content-preserving warps for 3d video stabilization. In *IEEE Conference on Computer Vision and Pattern Recognition*.

APPENDIX

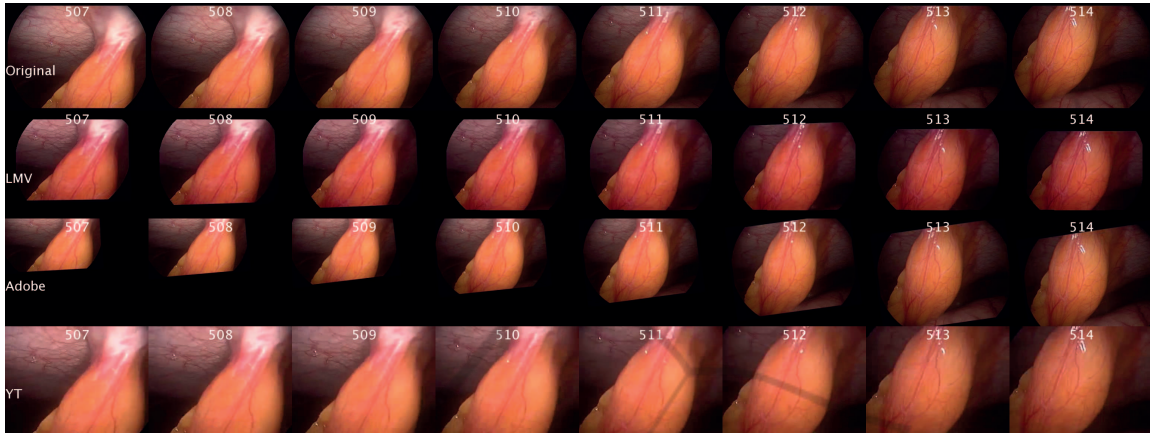


Figure 8: Comparison of the state-of-the-art algorithms for a stabilized scene having no foreground moving object.

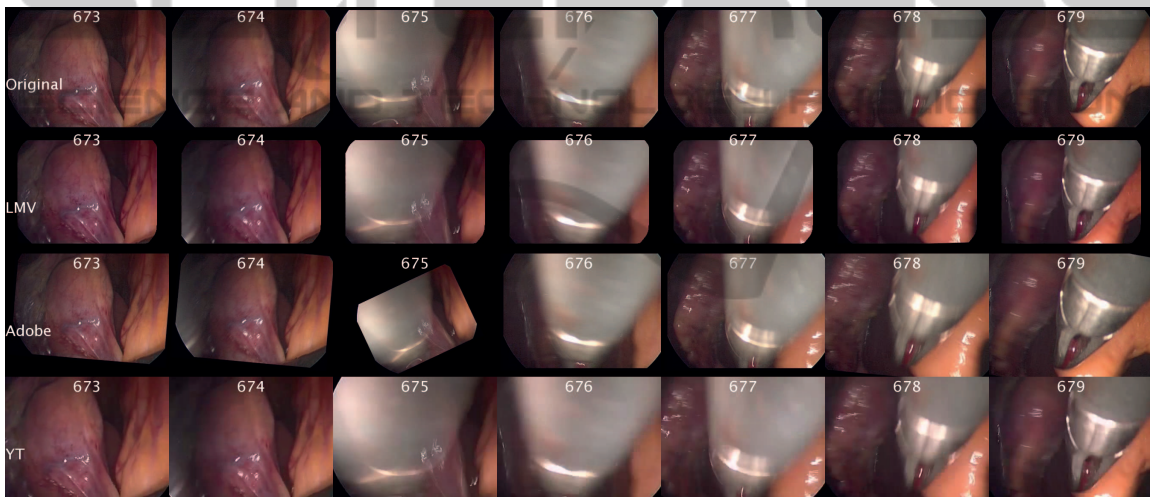


Figure 9: Comparison of the state-of-the-art algorithms for a stabilized scene having foreground moving object.

Table 1: List of the videos used for stabilization.

Video	Description
a	Bronchoscopic staboptoc video of a rat with circular content
b	Bronchoscopic staboptoc video of a rat with rectangular content and moving camera
c	Bronchoscopic staboptoc video of a rat with rectangular content and steady camera
d	Shaky video of a hippo
e	Human Rhinoscopic 1 with rectangular content and steady camera
f	Human Rhinoscopic 2 with rectangular content and steady camera
g	Human Rhinoscopic 3 with rectangular content and steady camera
h	Human surgery video with scalpel moving in the foreground
i	Lab video 1 with forward and backward movement
j	Lab video 2 with forward and backward movement
k	Bronchoscopic grid removed fibreoptic video of a rat with steady camera
l	Bronchoscopic grid removed fibreoptic video of a rat with moving camera and distortion (Bubbles)
m	Bronchoscopic grid removed fibreoptic video of a rat with forward-backward movement of camera
n	Bronchoscopic grid removed fibreoptic video of a rat with rectangular content and steady camera
o	Shaky video of a tiger with jittery motion

Table 2: Dataset 1- List of the videos used for Distortion-Specific stabilization.

Videos	Distortions	Frames
19	Foreground Objects	10981
12	Body Fluids	3283
23	Smoke	7754
23	Camera Shaking	6311
22	Shaking ROI	8333
23	Luminance Changes	7382
15	Body Movements	2815
15	Spotlights	5545
25	Low Contrast	6849
5	Dirty Lens	6150
2	Low Light	3601

